

# The Lyman $\alpha$ forest opacity and the metagalactic hydrogen ionization rate at $z \sim 2-4$

James S. Bolton,<sup>1\*</sup> Martin G. Haehnelt,<sup>1,2</sup> Matteo Viel<sup>1</sup> and Volker Springel<sup>3</sup>

<sup>1</sup>*Institute of Astronomy, University of Cambridge, Madingley Road, Cambridge CB3 0HA*

<sup>2</sup>*Kavli Institute for Theoretical Physics, University of California, Santa Barbara, CA 93106, USA*

<sup>3</sup>*Max-Planck-Institut für Astrophysik, Karl-Schwarzschild-Str. 1, Garching bei München, Germany*

Accepted 2004 December 1. Received 2004 November 25; in original form 2004 November 2

## ABSTRACT

Estimates of the metagalactic hydrogen ionization rate from the Ly $\alpha$  forest opacity in QSO absorption spectra depend on the complex density distribution of neutral hydrogen along the line of sight. We use a large suite of high-resolution hydrodynamical simulations to investigate in detail the dependence of such estimates on physical and numerical parameters in the context of  $\Lambda$ CDM models. Adopting fiducial values for cosmological parameters together with published values of the temperature of the IGM and the effective optical depth, the metagalactic ionization rates that reproduce the Ly $\alpha$  effective optical depth at  $z = [2, 3, 4]$  are  $\Gamma_{\text{HI}} = [1.3 \pm_{0.5}^{0.8}, 0.9 \pm 0.3, 1.0 \pm_{0.3}^{0.5}] \times 10^{-12} \text{ s}^{-1}$ , respectively. The errors include estimates of uncertainties in the relevant physical parameters and the numerical accuracy of the simulations. We find the errors are dominated by the uncertainty in the temperature of the low-density IGM. The estimated metagalactic hydrogen ionization rate for the neutral hydrogen distribution in the current concordance  $\Lambda$ CDM model is more than four times the value inferred for that in an Einstein–de Sitter model of the same rms-density-fluctuation amplitude  $\sigma_8$ . The estimated ionization rate is also more than double that expected from updated estimates of the emissivity of observed QSOs alone. A substantial contribution from galaxies appears to be required at all redshifts.

**Key words:** hydrodynamics – methods: numerical – intergalactic medium – quasars: absorption lines – diffuse radiation.

## 1 INTRODUCTION

In recent years, high-resolution, high signal-to-noise quasi-stellar object (QSO) spectra (e.g. Lu et al. 1996; Kirkman & Tytler 1997; Kim et al. 2002), combined with hydrodynamical simulations (Cen 1992; Zhang, Anninos & Norman 1995; Hernquist et al. 1996; Miralda Escudé et al. 1996; Theuns et al. 1998), have provided fresh insight into the nature of the intergalactic medium (IGM). It is now widely accepted that the Ly $\alpha$  forest arises from absorption by density fluctuations imposed on the warm photoionized IGM as suggested by analytical calculations (Bi, Börner & Chu 1992; Bi & Davidson 1997), and is a natural consequence of hierarchical structure formation within CDM-like models (see Rauch 1998, for a review).

One notable inconsistency with this paradigm has been the rather low values of  $\Gamma_{\text{HI}}$  inferred from early hydrodynamical simulations of the Ly $\alpha$  forest if scaled to appropriate assumptions for the IGM temperature (e.g. Rauch et al. 1997). However, the matter density

$\Omega_m$ , baryon density  $\Omega_b$ , amplitude of mass fluctuations  $\sigma_8$  and the parametrized Hubble constant  $h = H_0/100 \text{ km s}^{-1} \text{ Mpc}^{-1}$ , as well as the gas temperature and the Ly $\alpha$  effective optical depth,  $\tau_{\text{eff}} = -\ln \langle F \rangle_{\text{obs}}$ , all influence such an estimate. This has led to a wide range of estimates for  $\Gamma_{\text{HI}}$  inferred from the Ly $\alpha$  forest opacity using numerical simulations with different assumptions (Rauch et al. 1997; Theuns et al. 1998; Haehnelt et al. 2001; McDonald & Miralda-Escudé 2001; Hui et al. 2002; Meiksin & White 2003, 2004; Schaye et al. 2003; Sokasian, Abel & Hernquist 2003; Tytler et al. 2004). This complicates the comparison with determinations of the ionization rate from estimates of the integrated emission from observed QSOs and/or galaxies (e.g. Haardt & Madau 1996, hereafter HM96; Madau, Haardt & Rees 1999) and estimates using the proximity effect (e.g. Bajtlik, Duncan & Ostriker 1988; Bechtold 1994; Cooke, Espey & Carswell 1997; Scott et al. 2000) which both also have rather large uncertainties. Furthermore, Steidel, Pettini & Adelberger (2001), in a study of Lyman-break galaxies at  $z \simeq 3.4$ , suggested that the intensity of the ionizing background may be a factor of a few larger than in the model of HM96 owing to a large contribution from star-forming galaxies.

\*E-mail: jsb@ast.cam.ac.uk

In this paper we present new estimates of the metagalactic hydrogen ionization rate using Ly $\alpha$  forest opacity measurements taken from the literature. Our approach expands on previous studies in that we examine the dependence of  $\Gamma_{\text{HI}}$  upon the various cosmological and astrophysical parameters using a large suite of hydrodynamical simulations. In Section 2 we present an overview of our numerical code and our method for obtaining  $\Gamma_{\text{HI}}$  from artificial Ly $\alpha$  spectra. We examine how  $\Gamma_{\text{HI}}$  depends on a wide variety of parameters in Section 3, and compare our results to previous estimates using the same technique in Section 4. In Section 5 we present our best values for  $\Gamma_{-12}$  at  $z = [2, 3, 4]$  and consider the implications for sources of ionizing radiation. Section 6 contains our summary and conclusions.

## 2 FROM MEAN FLUX TO IONIZATION RATE

### 2.1 The fluctuating Gunn–Peterson approximation

At redshifts where the Ly $\alpha$  forest is commonly observed, density fluctuations in the low-density, unshocked baryons closely follow those of the underlying dark matter (Zhang et al. 1998). The balance between photoheating of unshocked gas and cooling due to the adiabatic expansion of the Universe results in a power-law temperature–density relation for the normalized gas density  $\Delta = \rho/\langle\rho\rangle \leq 10$ , where  $T = T_0\Delta^{\gamma-1}$  (Hui & Gnedin 1997). This is often referred to as the effective equation of state of the IGM, for which, typically,  $10^{3.7} \text{ K} \leq T_0 \leq 10^{4.3} \text{ K}$  and  $1.0 \leq \gamma \leq 1.6$ . Additionally, in photoionization equilibrium the Ly $\alpha$  optical depth,  $\tau$ , is proportional to the density of neutral hydrogen,  $n_{\text{HI}}$ . Neglecting collisional ionization, which is an acceptable approximation at the low-densities associated with Ly $\alpha$  forest absorbers,  $n_{\text{HI}} \propto \rho^2 T^{-0.7}/\Gamma_{\text{HI}}$ , where  $\rho$  is the gas density,  $T$  is the temperature and  $\Gamma_{\text{HI}}$  is the hydrogen ionization rate per atom. Combining these relations gives a simple power-law expression relating the optical depth of Ly $\alpha$  absorbers to the physical properties of the hydrogen gas (Weinberg et al. 1999). This relation has been termed the Fluctuating Gunn–Peterson Approximation (FGPA).

The optical depth due to Ly $\alpha$  absorption for a homogeneous distribution of hydrogen gas in an isotropically expanding Universe was discussed by Gunn & Peterson (1965). The FGPA applies to an inhomogeneous IGM in photoionization equilibrium. Ignoring the effect of peculiar velocities and thermal broadening, the optical depth to Ly $\alpha$  scattering is given by (e.g. Weinberg et al. 1999; McDonald & Miralda-Escudé 2001):

$$\tau = \tau_0 \frac{(1+z)^6 (\Omega_b h^2)^2}{T^{0.7} H(z) \Gamma_{-12}(z)} \Delta^\beta, \quad (1)$$

where  $\Omega_b$  is the baryonic matter density as a fraction of the critical density,  $h = H_0/100 \text{ km s}^{-1} \text{ Mpc}^{-1}$  for the present-day Hubble constant  $H_0$ ,  $T$  is the gas temperature at normalized density  $\Delta$ ,  $\Gamma_{-12}(z) = \Gamma_{\text{HI}}(z)/10^{-12} \text{ s}^{-1}$  at redshift  $z$  and  $\tau_0$  is a constant. The index  $\beta = 2 - 0.7(\gamma - 1)$  is determined by the slope of the effective equation of state, and asymptotically approaches  $\simeq 1.6$  after reionization. For a flat Universe at redshifts  $z \geq 2$  the Hubble parameter can be approximated by  $H(z) \simeq H_0 \Omega_m^{1/2} (1+z)^{3/2}$ . Thus, given the correct density distribution, velocity distribution and effective equation of state at redshift  $z$ , the Ly $\alpha$  optical depth should scale according to the parameter combination

$$\mu = \Omega_b^2 h^3 T^{-0.7} \Omega_m^{-0.5} \Gamma_{-12}^{-1} \quad (2)$$

for redshifts  $z \geq 2$  (Rauch et al. 1997). This assumes that thermal broadening and peculiar velocities will not have a large effect on

the optical depth distribution. At the densities and physical scales of the Ly $\alpha$  forest absorbers Hubble broadening is expected to be dominant (Weinberg et al. 1997), which should make this a reasonable assumption.

We match the mean flux of artificial Ly $\alpha$  spectra constructed from hydrodynamical simulations to observed values by linearly rescaling the simulated optical depths. If the FGPA approximation holds this corresponds to changing the parameter combination  $\mu$  by the same factor. We have determined  $\mu$  in this way. If independent estimates are available for  $\Omega_b$ ,  $\Omega_m$ ,  $h$ ,  $T$  and  $\tau_{\text{eff}}$ , the magnitude of  $\Gamma_{-12}$  required to reproduce the observed mean flux can be derived. This assumes that the effect of absorption by fully neutral gas on the mean flux level is small, which should again be a reasonable assumption.

### 2.2 Numerical code

We proceed to investigate how  $\Gamma_{-12}$  depends on several cosmological and astrophysical parameters using a suite of hydrodynamical simulations. The simulations were run using a new version of the parallel TreeSPH code GADGET (Springel, Yoshida & White 2001). GADGET-2 has the option of using a TreePM mode to perform the long-range gravitational computations, which results in a significant reduction in computational run-time.

The conservative entropy formulation of Springel & Hernquist (2002) is used to model the SPH particles, and radiative cooling is included using the prescription of Katz, Weinberg & Hernquist (1996). We have used the UV background specified by HM96 based on observed counts of QSOs, but with artificially increased heating rates to explore the effect of gas temperature on  $\Gamma_{-12}$ . Our fiducial model uses a heating rate a factor of 3.3 greater than the HM96 value in the optically thin limit, which results in temperatures close to those observed in the IGM (Bryan & Machacek 2000; Ricotti, Gnedin & Shull 2000; Schaye et al. 2000). The fiducial temperatures at mean gas density we shall assume are  $T_0 = [11200, 17800, 12500] \text{ K}$  at  $z = [2, 3, 4]$ , based on the results of Schaye et al. (2000) (which are consistent with He II reionization at  $z \simeq 3$ ). At present there are only weak observational constraints on the index  $\gamma$  of the temperature–density relation and its dependence on redshift (McDonald et al. 2001; Ricotti et al. 2000; Schaye et al. 2000). The plausible range is  $1 < \gamma < 1.6$  and in the following we will adopt  $\gamma = 1.3$  as the fiducial value. Unless otherwise noted, the temperatures of the gas have been rescaled such that the temperature at mean gas density  $T_0$  has the above fiducial values and the index of the power-law temperature–density relation for low gas densities is  $\gamma = 1.3$ . At higher gas densities the temperature–density relation asymptotes to  $T \simeq 10^4 \text{ K}$  as atomic cooling becomes important.

Star formation is included using a simplified prescription to maximize the speed of the simulations. All gas particles with  $\Delta > 10^3$  and  $T < 10^5 \text{ K}$  are converted into collisionless stars. Comparisons with identical simulations using the multi-phase model of Springel & Hernquist (2003) show little difference in the Ly $\alpha$  absorption (Viel, Haehnelt & Springel 2004b). Additionally, all GADGET-2 feedback options have been disabled. The effect of feedback from galactic winds on the flux distribution is uncertain but is believed to be small (e.g. Theuns et al. 2002; Bruscoli et al. 2003; Desjacques et al. 2004). Simulations run by one of us (VS) indicate that the inclusion of winds only marginally alters the opacity of the Ly $\alpha$  forest, such that the mean transmitted Ly $\alpha$  flux predicted by different models varies to less than half a per cent. There also appears to be no monotonic trend of the mean transmitted flux with wind strength. It is, however, conceivable that more realistic implementations of

**Table 1.** Parameters used in our suite of hydrodynamical simulations where we assume a flat Universe with  $\Omega_\Lambda = 1 - \Omega_m$ . The last column lists the photoheating rate as a factor of the HM96 value.

Name	$\Omega_m$	$\Omega_b h^2$	$h$	$\sigma_8$	$n$	UV
Fiducial	0.26	0.0240	0.72	0.85	0.95	3.3
T1	0.26	0.0240	0.72	0.85	0.95	0.3
T2	0.26	0.0240	0.72	0.85	0.95	1.0
T3	0.26	0.0240	0.72	0.85	0.95	2.0
T4	0.26	0.0240	0.72	0.85	0.95	4.0
M1	0.17	0.0240	0.72	0.85	0.95	3.3
M2	0.40	0.0240	0.72	0.85	0.95	3.3
M3	0.70	0.0240	0.72	0.85	0.95	3.3
M4	1.00	0.0240	0.72	0.85	0.95	3.3
S1	0.26	0.0240	0.72	0.50	0.95	3.3
S2	0.26	0.0240	0.72	0.70	0.95	3.3
S3	0.26	0.0240	0.72	1.00	0.95	3.3
S4	0.26	0.0240	0.72	1.20	0.95	3.3
$\Lambda$ CDM	0.40	0.0150	0.65	0.79	0.95	3.3
SCDM	1.00	0.0125	0.50	0.70	1.00	1.0

galactic winds within our simulations may lead to a multi-phase medium with dense cool clouds, which may increase the Ly $\alpha$  forest opacity and thus the estimated hydrogen ionization rate. We neglect this possibility in this work. Note that Theuns et al. (2002) find the inclusion of winds alters the mean transmission by 10 per cent.

The simulation parameters are listed in Table 1. For each model we have run a simulation with  $200^3$  dark matter particles and  $200^3$  gas particles within a  $15h^{-1}$  comoving Mpc box having periodic boundary conditions. We find this to be the best compromise between accuracy and speed for our parameter study. For our fiducial model we have also run simulations with different box sizes and mass resolutions to test numerical convergence (see Section 2.4). These are listed in Table 2. Note that the simulations with  $200^3$  particles used for the parameter study do not give fully converged estimates of  $\Gamma_{-12}$  and we will later show results corrected for box size and resolution. In addition, we have run  $\Lambda$ CDM and SCDM simulations with  $2 \times 64^3$  particles and box sizes of 10- and  $11.1h^{-1}$  comoving Mpc, respectively, to mimic the simulations used in the seminal study of Rauch et al. (1997). The parameters are also listed in Table 1.

The simulations were started at  $z = 99$ , with initial conditions generated using the CDM transfer functions of Eisenstein & Hu (1999). The initial gas temperature was  $T = 227$  K and the gravitational softening length was  $2.5h^{-1}$  comoving kpc. The simulations were run on COSMOS, a 152 Gb shared memory Altix 3700 with

**Table 2.** Resolution and box size of our six additional simulations which have the same parameters as the 15–200 model used for our parameter study. The mass resolution used for our parameter study is also listed for comparison.

Name	Box size comoving Mpc	SPH particles	Mass resolution $h^{-1} M_\odot/\text{gas particle}$
15–400	$15 h^{-1}$	$400^3$	$6.78 \times 10^5$
30–400	$30 h^{-1}$	$400^3$	$5.42 \times 10^6$
15–100	$15 h^{-1}$	$100^3$	$4.34 \times 10^7$
30–200	$30 h^{-1}$	$200^3$	$4.34 \times 10^7$
60–400	$60 h^{-1}$	$400^3$	$4.34 \times 10^7$
30–100	$30 h^{-1}$	$100^3$	$3.47 \times 10^8$
15–200	$15 h^{-1}$	$200^3$	$5.42 \times 10^6$

152 1.3-GHz Itanium2 processors hosted by the Department of Applied Mathematics and Theoretical Physics (Cambridge).

### 2.3 Method for determining $\Gamma_{-12}$ from simulations

Artificial Ly $\alpha$  spectra are constructed at  $z = [2, 3, 4]$  from 1024 random lines of sight (LOSs) parallel to the box boundaries (e.g. Theuns et al. 1998). Each LOS consists of 1024 pixels. We mimic the noise on high-resolution QSO spectra by adding Gaussian distributed noise with a total S/N of 30. The simulated optical depths we use are divided by a constant factor of 1.225 to correct the hydrogen recombination coefficient  $\alpha_{\text{HI}}$  used in our simulations, which is taken from Cen (1992). As noted by Rauch et al., this value of  $\alpha_{\text{HI}}$  is around 20 per cent larger than the calculation of Abel et al. (1997) within the relevant temperature range for unsaturated absorption in the Ly $\alpha$  forest. Abel et al. base their fit for  $\alpha_{\text{HI}}$  on the data of Ferland et al. (1992).

To determine  $\Gamma_{-12}$  we rescale the optical depths of the artificial spectra to match the mean observed flux of the Ly $\alpha$  forest at  $z = [2, 3, 4]$ . We use the central values of  $\tau_{\text{eff}}$  from the fitting formula of Schaye et al. (2003), based on a sample of 19 high-resolution QSO spectra, such that  $\langle F \rangle_{\text{obs}} = e^{-\tau_{\text{eff}}} = [0.878 \pm 0.019, 0.696 \pm 0.025, 0.447 \pm 0.031]$ . The uncertainties on these values were estimated by binning the  $1\sigma$  errors in  $\tau_{\text{eff}}$  presented in table 5 of Schaye et al. (2003) into redshift bins of width  $\Delta z = 0.5$ . These values have been corrected for absorption from metal lines and Ly $\alpha$  systems with damping wings. We rescale the optical depth in each pixel by a constant factor  $A$  to reproduce  $\langle F \rangle_{\text{obs}}$  at the appropriate redshift. Hence, for a set of spectra with a total of  $N$  pixels,

$$\langle F \rangle_{\text{obs}} = \frac{1}{N} \sum_{j=1}^N e^{-A\tau_j} = e^{-\tau_{\text{eff}}}, \quad (3)$$

where  $\tau_j$  is optical depth in each pixel of the simulated spectra. The value of  $\Gamma_{-12}$  required to reproduce  $\langle F \rangle_{\text{obs}}$  from the simulated spectra is then calculated.

### 2.4 The effect of box size and mass resolution on the ionization rate

We first vary the box size and resolution of simulations of our fiducial model to assess their effect on the value of  $\Gamma_{-12}$ . The simulation box must be large enough to include long wavelength density perturbations and represent a fair sample of the Universe while retaining adequate resolution. The left panel of Fig. 1 shows  $\Gamma_{-12}$  for different box sizes at fixed mass resolution. As the box size increases, the simulated optical depths decrease; low-density gas responsible for Ly $\alpha$  absorption falls into the haloes formed in the simulation, producing larger and emptier voids. A smaller  $\Gamma_{-12}$  is thus required to reproduce the observed optical depth. The data have almost converged for a box size of  $30h^{-1}$  comoving Mpc, with a difference of less than 2 per cent between the  $\Gamma_{-12}$  inferred from the 60–400 and 30–200 models.

The right panel illustrates the effect of changing the mass resolution on  $\Gamma_{-12}$  for fixed box sizes of 15- and  $30h^{-1}$  comoving Mpc. Increasing the mass resolution decreases the optical depth because higher-resolution simulations resolve smaller haloes. More gas is taken from the low-density IGM and a smaller value of  $\Gamma_{-12}$  is required to match the observed mean flux. Simulations with less than  $400^3$  gas particles within a  $30h^{-1}$  comoving Mpc box do not achieve adequate numerical convergence. The difference between  $\Gamma_{-12}$  calculated from the  $200^3$  and  $400^3$  simulations is on average

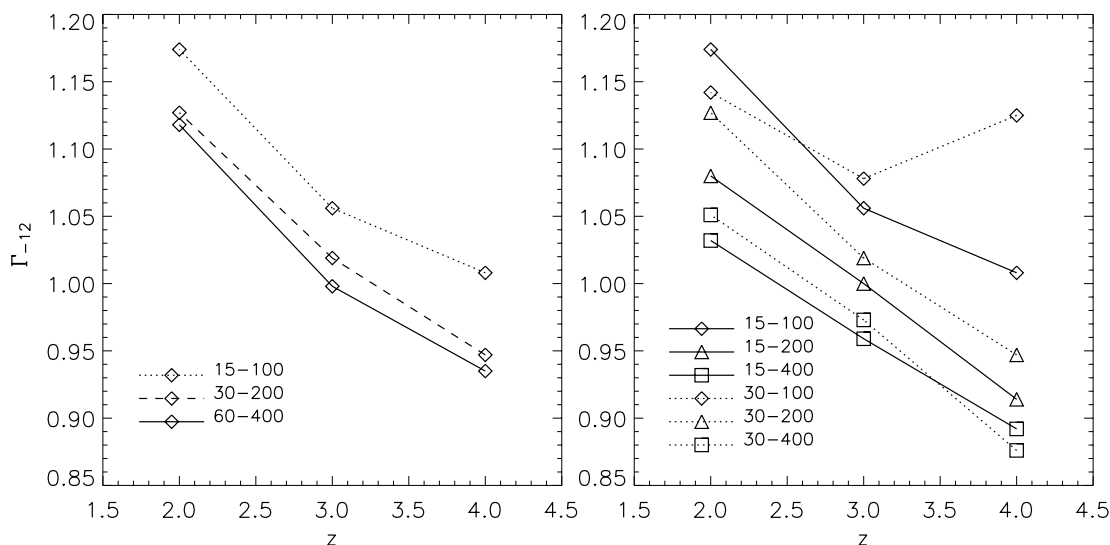


**Figure 1.** The effect of box size (left panel) and mass resolution (right panel) on the estimated  $\Gamma_{-12}$  (see Table 2). The model parameters are those of the fiducial model (see Table 1).

7 per cent. Comparison of the simulation with  $200^3$  and  $400^3$  particles within a  $15-h^{-1}$  comoving Mpc box shows that a further increase in resolution reduces  $\Gamma_{-12}$  by an extra 5 per cent.

Unfortunately,  $400^3$  simulations are too computationally expensive for the purpose of exploring a large parameter space. We compromise by taking our fiducial model to have  $200^3$  gas particles within a  $15-h^{-1}$  comoving Mpc box; the value of  $\Gamma_{-12}$  we infer will be systematically high by around 8 per cent due to the combined error from box size and resolution. Hereafter, all results based on simulations with  $200^3$  particles within a  $15-h^{-1}$  comoving Mpc box will be reduced by this factor to correct for box size and resolution. Note that this correction is likely to be a lower limit to the true correction required; our highest-resolution simulations may not yet have reached numerical convergence. We will account for this uncertainty in our error analysis in Section 5.1.

### 3 SCALING RELATIONS FOR $\Gamma_{-12}$ FROM SIMULATED ABSORPTION SPECTRA

It is implicit in the FGPA scaling relation that the density and velocity distribution, along with the effective equation of state of the Ly $\alpha$  absorbers, remain unchanged for different values of  $\Omega_b$ ,  $h$ ,  $\Omega_m$ ,  $T$  and  $\Gamma_{-12}$ . Hence, when inferring  $\Gamma_{-12}$  from hydrodynamical simulations and subsequently rescaling with different parameters, it is generally assumed that

$$\Gamma_{-12} \propto \Omega_b^2 h^3 T^{-0.7} \Omega_m^{-0.5} \quad (4)$$

(e.g. Rauch et al. 1997; McDonald & Miralda-Escudé 2001). However, it is not clear if this relation is an accurate approximation. Altering  $\Omega_m$  is likely to alter the gas-density distribution, and thermal broadening may produce a deviation from the  $T^{-0.7}$  scaling based on the temperature dependence of the recombination coefficient. In addition, the dependence of  $\Gamma_{-12}$  on the polytropic index  $\gamma$  of the effective equation of state  $T = T_0 \Delta^{\gamma-1}$  is unclear. Although hydrodynamical simulations predict  $\gamma \simeq 1.6$  at low density, if He II reionization occurs at  $z \simeq 3$  (Reimers et al. 1997; Schaye et al. 2000; Bernardi et al. 2003) the effective equation of state for the low-density gas may become isothermal. Radiative transfer effects may also raise the temperature of the gas and blur the monotonic

relation between temperature and density (Abel & Haehnelt 1999; Bolton, Meiksin & White 2004). Finally, changing  $\sigma_8$  will affect  $\Gamma_{-12}$  by changing the density distribution of the gas.

We test the validity of equation (4) using our suite of hydrodynamical simulations. The motivation for this is two-fold: first, it is important to understand the physical processes which alter the value of  $\Gamma_{-12}$  that we infer from simulations; secondly, we wish to determine how  $\Gamma_{-12}$  scales with the input parameters, allowing us to place joint constraints upon them. We do not discuss the scaling with  $\Omega_b$  and  $h$ , since our analysis revealed that the FGPA scaling relation holds extremely well for these parameters.

#### 3.1 The dependence of $\Gamma_{-12}$ on temperature

The left panel of Fig. 2 shows our test of the FGPA scaling relation for the gas temperature at mean density using five simulations with photoheating rates [0.3, 1.0, 2.0, 3.3, 4.0] times the HM96 values. We expect the ionization rate to decrease as the HM96 photoheating rate is raised; the hydrogen recombination rate scales as  $T^{-0.7}$ , so for larger temperatures there is less neutral hydrogen. We find a modest deviation from the  $T^{-0.7}$  scaling (shown as the dotted curves) at low temperatures, probably due to thermal broadening of absorption features, an effect that is strongest at  $z = 4$ . The fiducial model with its higher gas temperatures will have relatively broader absorption features, producing more Ly $\alpha$  absorption and thus requiring a larger value of  $\Gamma_{-12}$  than if thermal broadening were absent. The FGPA scaling relation for the fiducial model will slightly overpredict the value of  $\Gamma_{-12}$  at lower temperatures. The same process also occurs for gas temperatures higher than the fiducial model; the absorbers are thermally broadened to a greater extent so the scaling relation underpredicts the ionization rate. This effect is much more apparent at higher redshifts when the spatial density of Ly $\alpha$  absorbers is greater. Note that the temperature dependence of the gas pressure may also contribute to the deviation from  $T^{-0.7}$  scaling. We perform a least-squares fit on the data to obtain the following scaling for  $\Gamma_{-12}$  with temperature:

$$\Gamma_{-12} \propto T^{x_1(z)}, \quad (5)$$

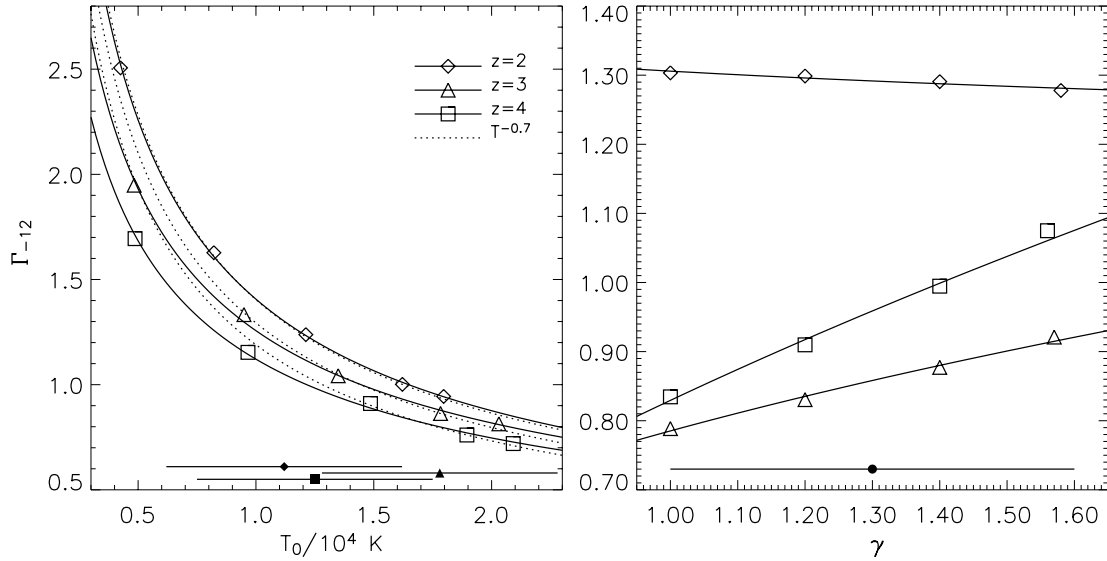


**Figure 2.** *Left:* the dependence of  $\Gamma_{-12}$  on the gas temperature at mean density  $T_0$  at three different redshifts as indicated on the plot. Results are corrected for box size and resolution as discussed in Section 2.4. Solid curves show a least-squares fit and the dotted curves shows the  $T^{-0.7}$  scaling due to the temperature dependence of the recombination coefficient. The filled symbols show the fiducial temperatures and their uncertainties. *Right:* the dependence of  $\Gamma_{-12}$  on the index of the temperature density relation  $\gamma$ . Results are corrected for box size and resolution. The filled circle shows our fiducial value of  $\gamma$  and its uncertainty.

where  $x_1(z) = [-0.68, -0.62, -0.59]$  at  $z = [2, 3, 4]$ . We shall adopt these scaling relations (shown as solid curves) from here onwards.

### 3.2 The dependence of $\Gamma_{-12}$ on $\gamma$

The dependence of the hydrogen ionization rate on the polytropic index  $\gamma$  is shown in the right panel of Fig. 2. The value of  $\gamma$  is varied by artificially rescaling the effective equation of state of our existing fiducial simulation data by pivoting the temperature–density relation around the mean gas density (Viel et al. 2004b). Note that the actual slope of the effective equation of state predicted by the numerical simulations is  $\gamma \simeq 1.6$ . This will not account for any dynamical effects the different temperatures have on the gas distribution, but it will model thermal broadening and the change in neutral hydrogen density correctly, thus providing a reasonable approximation. Note that the data point with the largest  $\gamma$  is for our simulation of the fiducial model with no scaling of  $\gamma$ . It is clear from Fig. 2 that the inferred ionization rate has a non-negligible dependence on  $\gamma$ . At  $z = 3$  and  $z = 4$ ,  $\Gamma_{-12}$  increases with  $\gamma$ . A flatter effective equation of state produces hotter gas at densities less than the cosmic mean with a lower neutral hydrogen fraction. As most of the Ly $\alpha$  absorption is produced by this gas, decreasing  $\gamma$  will decrease the amount of absorption and hence lower the inferred ionization rate. The dependence of  $\Gamma_{-12}$  on  $\gamma$  is much stronger at  $z = 4$  compared to  $z = 3$ . However, at  $z = 2$ , the trend is the opposite: the ionization rate decreases with increasing  $\gamma$ , albeit with a weak dependence. This can be explained by considering the density evolution of the Ly $\alpha$  absorbers. With decreasing redshift, the mean gas density decreases. By  $z = 2$ , the optical depth in regions of average density and below has become so low that these contribute very little to the overall effective optical depth. The absorption is almost entirely due to overdense regions. Decreasing the polytropic index will lower the temperature of this gas, increasing the neutral hydrogen fraction and slightly increasing the effective optical depth. The inferred ionization rate increases slightly with decreasing  $\gamma$  as a consequence. In a similar manner to before, we perform a least-squares fit on the data

to obtain a scaling relation for the ionization rate with the polytropic index  $\gamma$ :

$$\Gamma_{-12} \propto \gamma^{x_2(z)}, \quad (6)$$

where  $x_2(z) = [-0.04, 0.34, 0.55]$  at  $z = [2, 3, 4]$ . These scaling relations are shown in Fig. 2 as the solid curves.

### 3.3 The dependence of $\Gamma_{-12}$ on $\Omega_m$

The FGPA scaling relation assumes that the ionization rate per atom scales as  $\Omega_m^{-0.5}$ . For this to be true, the density distribution of the neutral hydrogen gas must remain the same for different values of  $\Omega_m$ . We test this scaling relation using five simulations with  $\Omega_m = [0.17, 0.26, 0.4, 0.7, 1.0]$  and show the results in the left panel of Fig. 3. As before, the plotted values are rescaled to match the fiducial temperatures,  $\gamma = 1.3$ , corrected for box size and resolution and are shown with the best-fitting curves to the data. The  $\Omega_m^{-0.5}$  scaling around the fiducial model is indicated by the dotted lines. This becomes a poorer fit to the data as  $\Omega_m$  is increased, and overestimates the value of  $\Gamma_{-12}$  substantially. It is worth stressing that all the models shown in the left panel of Fig. 3 have the same normalization at a scale of  $8 h^{-1}$  Mpc for the dark matter linear power spectrum ( $\sigma_8 = 0.85$ ). In order to understand why the discrepancy with the expected trend is so big we performed a new run for the Einstein–de Sitter (M4) model and normalized the power spectrum to have the same fluctuation amplitude as the fiducial model at the scale of  $30 \text{ km s}^{-1}$ , roughly corresponding to the Jeans length. The filled points in the left panel of Fig. 3 indicate the new values of  $\Gamma_{-12}$  we infer; one can see that these values are in better agreement with the theoretical curve, showing that  $\Gamma_{-12}$  is more sensitive to the rms fluctuations on a fixed velocity scale. This suggests that the rms-fluctuation amplitude at the Jeans scale is more relevant.

Fig. 4 shows the probability density function (PDF) of the volume weighted gas density as a fraction of the mean at  $z = 2$  for our fiducial model and the Einstein–de Sitter (M4) model. The density distribution of the Einstein–de Sitter model peaks at lower density,

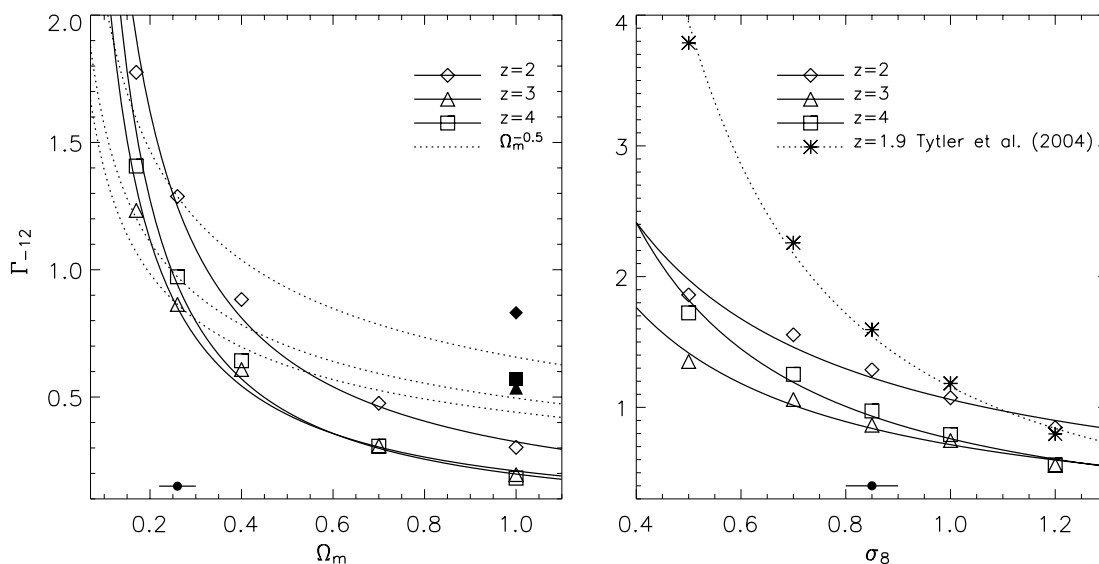


**Figure 3.** *Left:* the dependence of the estimated  $\Gamma_{-12}$  on  $\Omega_m$  for three different redshifts as indicated on the plot. The solid curves are a least-squares fit. The dotted lines show the  $\Omega_m^{-0.5}$  scaling. Filled points are obtained for a model with  $\Omega_m = 1.0$  and the same rms-fluctuation amplitude at a scale of  $30 \text{ km s}^{-1}$  as our fiducial model with  $\Omega_m = 0.26$ . As before the values are corrected for box size and resolution. The filled circle shows our fiducial value of  $\Omega_m = 0.26$  and its uncertainty. *Right:* the dependence of  $\Gamma_{-12}$  on  $\sigma_8$ . The dotted curve shows the result of Tytler et al. at  $z = 1.9$ , assuming  $\langle F \rangle_{\text{obs}} = 0.882 \pm 0.01$ . Results are corrected for box size and resolution. The filled circle shows our fiducial value of  $\sigma_8$  and its uncertainty.

explaining the much lower  $\Gamma_{-12}$  required to match the observed mean flux. In the Einstein–de Sitter model a greater proportion of the gas has fallen into haloes. Different gas-density distributions are not accounted for in the FGPA scaling relation. Comparisons of parameters such as  $\Gamma_{-12}$  and  $\Omega_b h^2$  inferred from simulations with different matter distributions using the FGPA gives misleading results. A least-squares fit to our data yields

$$\Gamma_{-12} \propto \Omega_m^{x_3(z)}, \quad (7)$$

where  $x_3(z) = [-1.00, -1.04, -1.16]$  at  $z = [2, 3, 4]$ .

### 3.4 The dependence of $\Gamma_{-12}$ on $\sigma_8$

The magnitude of  $\sigma_8$ , the mass fluctuation amplitude within  $8 h^{-1}$  Mpc spheres, also alters the required  $\Gamma_{-12}$ . For small  $\sigma_8$ , there is less small-scale power and the collapse of structures is less advanced. This produces a narrower volume weighted density PDF with a larger average density. This decreases the mean flux of the simulated spectra if the ionization rate is kept fixed. A larger  $\Gamma_{-12}$  is thus required to reproduce the observed effective optical depth.

The right panel of Fig. 3 shows  $\Gamma_{-12}$  for  $\sigma_8 = [0.5, 0.7, 0.85, 1.0, 1.2]$  at redshifts  $z = [2, 3, 4]$ . Tytler et al. (2004) present a similar plot in their fig. 16, where they construct curves relating  $\sigma_8$  and  $\gamma_{912} = \Gamma_{-12}/1.329$ , normalized to the predicted ionization rate at  $z = 1.9$  from Madau et al. (1999). The central curve in their plot gives the  $\Gamma_{-12}$  and  $\sigma_8$  they require to reproduce  $\langle F \rangle_{\text{obs}} = 0.882 \pm 0.01$ . We find a weaker dependence of  $\Gamma_{-12}$  on  $\sigma_8$ . We use similar values for  $\Omega_m$ ,  $h$ ,  $\Omega_b$ , the UV heating rate, and the slightly lower value of  $\tau_{\text{eff}}$ , which Tytler et al. use, will change our results only by a small amount (see Section 3.5). The small difference in redshift should also not alter the results significantly, and the resolution and box size of our simulations will also not account for the difference; increasing these systematically lowers  $\Gamma_{-12}$ . The most likely reason for this discrepancy is differences in the modelling techniques for our respective cosmological simulations (O’Shea et al. 2003). Tytler et al. use the Eulerian code ENZO (Norman & Bryan 1999). This

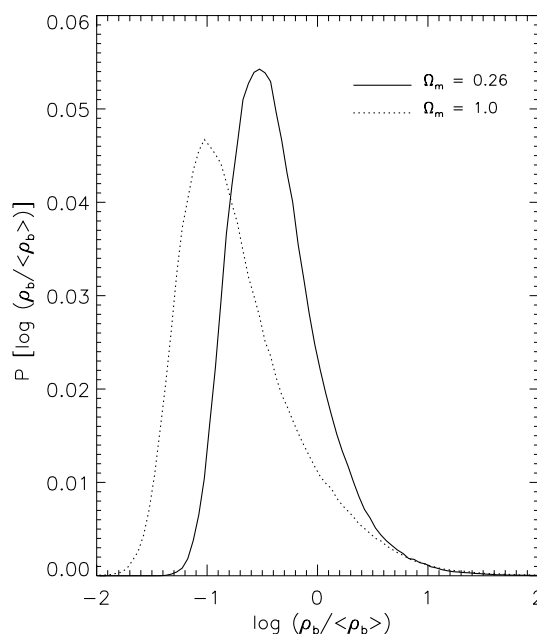


**Figure 4.** The PDF of the volume weighted gas density as a fraction of the mean at  $z = 2$  for the fiducial  $\Omega_m = 0.26$  (solid line) and M4  $\Omega_m = 1.0$  (dotted line) models. The fiducial model has a gas-density distribution that peaks at a greater amplitude closer to the mean density, producing more Ly $\alpha$  absorption at fixed  $\Gamma_{-12}$ .

models the gas component using a piecewise parabolic method, whereas we use a Lagrangian SPH code. A least-squares fit to our results gives

$$\Gamma_{-12} \propto \sigma_8^{x_4(z)}, \quad (8)$$

where  $x_4(z) = [-0.90, -0.99, -1.26]$  at  $z = [2, 3, 4]$ .

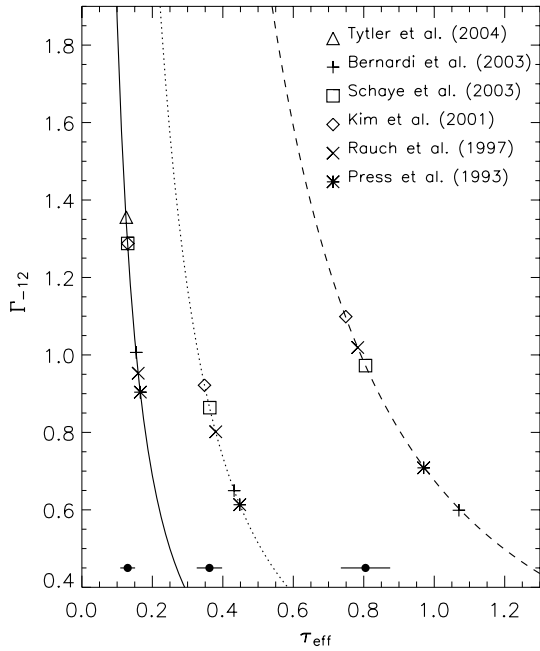


**Figure 5.** The dependence of  $\Gamma_{-12}$  on the effective optical depth at different redshifts for our fiducial model with our fiducial values of  $T_0$  and  $\gamma$ . The symbols indicate the values of  $\tau_{\text{eff}}$  quoted by various authors. The  $\tau_{\text{eff}}$  from Tytler et al. (2004) is for  $z = 1.9$ . The filled circles indicate our fiducial parameter values, with the estimated uncertainty shown by the horizontal line.

### 3.5 The dependence of $\Gamma_{-12}$ on $\tau_{\text{eff}}$

To determine the intensity and evolution of  $\Gamma_{-12}$  using the FGPA we must assume a value for the effective optical depth,  $\tau_{\text{eff}} = -\ln \langle F \rangle_{\text{obs}}$ . Measurements of the effective optical depths have been made by a number of authors (e.g. Press, Rybicki & Schneider 1993; Kim, Cristiani & D’Odorico 2001; Songalia & Cowie 2002; Bernardi et al. 2003; Schaye et al. 2003). The values obtained from low-resolution, low-S/N data by Press et al. and Bernardi et al. appear to be systematically higher than those obtained by the other groups, mainly from high-resolution data (see Viel et al. 2004b, for a discussion). The differences are primarily due to the systematic uncertainties in the continuum fits. Tytler et al. make an analysis of continuum fitting errors by comparing the true and fitted continua for sets of artificial spectra. They find that they can obtain a fit that is on average good to within 1–2 per cent, except for very low S/N spectra. Some agreement is emerging that the lower values from the higher-quality data are more appropriate. Statistical errors from the presence of metal absorption features and high column density absorbers also contribute to the uncertainty in  $\tau_{\text{eff}}$  (Viel et al. 2004a).

Fig. 5 shows the value of  $\Gamma_{-12}$  we infer from our fiducial model at  $z = [2, 3, 4]$  by varying the effective optical depth, and hence mean observed flux, to which the simulated optical depths are scaled to match. At  $z = 2$ , a change in  $\tau_{\text{eff}}$  of 0.05, which is consistent with the variation in estimates, results in almost a factor of two difference in the required hydrogen ionization rate. An accurate estimate of  $\tau_{\text{eff}}$  and the errors associated with the measurement are required to determine  $\Gamma_{-12}$ ; at  $z = 2$  even a small change in the assumed  $\tau_{\text{eff}}$  will change the inferred ionization rate appreciably. The best-fitting curve to the data is

$$\Gamma_{-12} \propto \tau_{\text{eff}}^{x_5(z)}, \quad (9)$$

where  $x_5(z) = [-1.44, -1.61, -1.68]$  at  $z = [2, 3, 4]$ .

## 4 COMPARISON WITH PREVIOUS ESTIMATES FROM SIMULATIONS

### 4.1 Hydrodynamical codes

In this section we shall make a direct comparison between our data and the results of other authors. First, we consider two simulations which are similar to the  $\Lambda$ CDM and SCDM models analysed by Rauch et al. (1997). The simulations have identical cosmological parameters, box size and resolution. Our  $\Lambda$ CDM model differs from that analysed by Rauch et al., since we use an SPH code rather than an Eulerian grid code. We try to approximate the different temperatures of the models by increasing the photoheating rate to 3.3 times the HM96 value for our  $\Lambda$ CDM simulation. This results in temperatures similar to those given by Rauch et al. at  $z = 2$  (this is the only redshift for which the temperature was published). The optical depths of our artificial spectra are scaled to match the mean flux used by Rauch et al., corrected for continuum fitting:  $\langle F \rangle_{\text{obs}} = [0.848, 0.670, 0.414]$  and  $[0.846, 0.655, 0.383]$  at  $z = [2, 3, 4]$  for the  $\Lambda$ CDM and SCDM models, respectively. Mimicking Rauch et al., we rescale  $\Gamma_{-12}$  by a factor  $(\Omega_b h^2)^2$ , setting  $\Omega_b h^2 = 0.024$ . Unlike in the rest of the paper, we have not corrected our data for numerical effects or rescaled the temperatures to match our fiducial values of  $T_0$  and  $\gamma$ .

Fig. 6 shows the redshift dependence of  $\Gamma_{-12}$  inferred from the  $\Lambda$ CDM and SCDM models as diamonds and triangles, respectively. The solid lines give our data and the Rauch et al. data are plotted as dotted lines. Rauch et al. conclude the large difference between  $\Gamma_{-12}$  obtained using the  $\Lambda$ CDM and SCDM models is primarily due to different gas temperatures in the respective simulations. The gas temperature at mean density in their SCDM model is about half that in the  $\Lambda$ CDM model at  $z = 2$ . We suggest the values of  $\Omega_m$ ,  $\sigma_8$  and  $\gamma$  used in each of the simulations will also alter  $\Gamma_{-12}$ . The different amounts by which the optical depths of the artificial

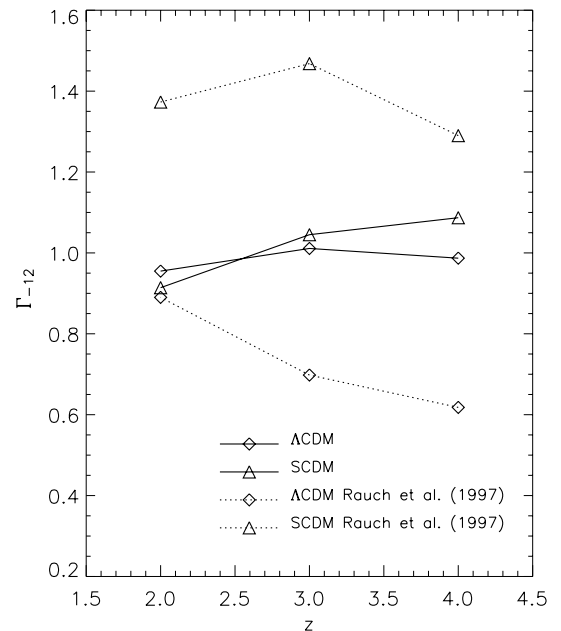


**Figure 6.** Comparison of the ionization rate inferred from GADGET-2 with that inferred from the simulations used in Rauch et al. (1997). Diamonds and triangles represent the  $\Lambda$ CDM and SCDM models, respectively. The GADGET-2 results are shown with solid lines while the results from Rauch et al. are shown with dotted lines.

spectra are scaled will also produce a small difference in  $\Gamma_{-12}$ , but this change will be negligible compared to the effect of the other parameters. In our simulations, the smaller temperature of the SCDM simulation counteracts the effect of different  $\Omega_m$  and  $\sigma_8$  and we find rather similar values for both simulations. The values for our  $\Lambda$ CDM simulation are larger than those in Rauch et al. while those for the SCDM simulation are smaller. Unfortunately the only information about the thermal state of the gas provided by Rauch et al. is at  $z = 2$ , which makes accurate comparison difficult. Although we attempt to match the gas temperature in our models at  $z = 2$  to those given by Rauch et al., this agreement is probably not good at higher redshifts, particularly for the  $\Lambda$ CDM model. The gas temperatures of the Rauch et al. models result from different reionization histories instead of artificially increased photoheating rates. The UV background of their  $\Lambda$ CDM model ionizes He II at  $z \simeq 3$ , which may lower the polytropic index  $\gamma$ . The  $\gamma$  in the Rauch et al.  $\Lambda$ CDM simulation may thus have been lower than that in our simulations. This would make the discrepancy smaller.

Schaye et al. (2003) utilize a hydrodynamical simulation based on a modified version of the SPH code HYDRA (Couchman, Thomas & Pearce 1995) to examine the metallicity of the IGM. Their model consists of a periodic box of  $12-h^{-1}$  comoving Mpc with  $256^3$  dark matter particles and  $256^3$  gas particles. The parameters they adopt are  $\Omega_m = 0.3$ ,  $\Omega_b h^2 = 0.019$ ,  $h = 0.65$ ,  $\sigma_8 = 0.9$  and  $n = 1.0$  with a UV background designed to reproduce the effective equation of state constrained by Schaye et al. (2000). The optical depths of the artificial Ly $\alpha$  spectra are scaled to match the same mean flux as ours. They find the  $\Gamma_{-12}$  required to match the mean flux of the Ly $\alpha$  forest at  $z = [2, 3, 4]$  are  $\Gamma_{-12} = [0.87, 0.54, 0.36]$ . Rescaling our fiducial model values of  $\Gamma_{-12} = [1.29, 0.86, 0.97]$  to match the cosmological parameters used by Schaye et al. reduces our values by around 40 per cent to  $\Gamma_{-12} = [0.80, 0.53, 0.57]$ . We remove the correction for box size and resolution from these values to allow a fair comparison. These are consistent with Schaye et al. (2003), allowing for the unknown differences between the exact thermal state of the low-density gas in the two simulations. Theuns, Schaye & Haehnelt (2000) also run simulations using HYDRA to study the broadening of Ly $\alpha$  absorption lines in QSO spectra. Their reference model consists of  $64^3$  dark matter particles and  $64^3$  gas particles within a periodic box of  $2.5-h^{-1}$  comoving Mpc, with the same cosmological parameters used by Schaye et al. and the UV background specified by Haardt & Madau (1996). This produces a temperature of  $T_0 \simeq 11\,750$  K at mean cosmic density. To reproduce an effective optical depth of  $\tau_{\text{eff}} = 0.33$  at  $z = 3$  they require  $\Gamma_{-12} = 0.87$ , based on the value of  $A$  quoted in their paper. Scaling our fiducial data to match their parameters reduces our value by 10 per cent to  $\Gamma_{-12} = 0.79$ . Although the mass resolution of our simulations is comparable, we obtain a smaller value because of our larger simulation box size.

Most recently, Tytler et al. (2004) made a detailed analysis of the Ly $\alpha$  forest at  $z = 1.9$ , using a set of 77 moderate resolution QSO spectra and compared it to a large hydrodynamical simulation run with the Eulerian code ENZO. Including uncertainties on the value of  $\sigma_8$ ,  $\Omega_b$  and  $\tau_{\text{eff}}$ , they find a joint constraint of  $\Gamma_{-12} = 1.44 \pm 0.36$ . They use a hydrodynamical simulation on a  $1024^3$  grid in a  $54.528-h^{-1}$  comoving Mpc box, with  $\Omega_m = 0.27$ ,  $\Omega_b h^2 = 0.022$ ,  $h = 0.71$ ,  $\sigma_8 = 0.9$  and  $n = 1.0$  and a UV background specified by Madau et al. (1999) with an artificially increased He II photoheating rate. Our fiducial result at  $z = 2$  rescaled to match the cosmological parameters and  $\tau_{\text{eff}} = 0.126$  at  $z = 1.9$  assumed by Tytler et al. gives  $\Gamma_{-12} = 1.17$ . This value is in reasonable agreement with the Tytler et al. result, again allowing for differences between the exact gas

temperatures and the numerical method. Note, however, that Tytler et al. found a different scaling of  $\Gamma_{-12}$  with  $\sigma_8$  (see Section 3.4 for details).

## 4.2 Pseudo-hydrodynamical codes

Several authors have also considered this problem using pseudo-hydrodynamical codes (e.g. Gnedin 1998; Gnedin & Hui 1998; Meiksin & White 2003, 2004). These approximate methods sacrifice accuracy for speed, allowing a much larger parameter space to be explored. Providing the accuracy of these approximations and the parameter ranges they model effectively are well controlled, they can provide an alternative method for modelling the IGM. Gnedin (1998) concludes that observational constraints on the column density distribution of the Ly $\alpha$  forest are consistent with the intensity of the UV background remaining constant in the redshift range  $z \sim 2-4$ . Meiksin & White (2004), in a study of UV background fluctuations, find the mean flux of the IGM is reproduced with  $\Gamma_{-12} = [0.88^{+0.14}_{-0.12}, 0.76^{+0.12}_{-0.11}]$  at  $z = [3, 4]$ . They adopt  $\Omega_m = 0.3$ ,  $\Omega_b h^2 = 0.020$ ,  $h = 0.70$ ,  $\sigma_8 = 1.0$  and  $n = 1.0$ , and impose an effective equation of state with  $T_0 = 20\,000$  K and  $\gamma = 1.5$ . Meiksin & White (2001) find that the spectral properties of the Ly $\alpha$  forest obtained from their code are reproduced to within 10 per cent of those found using fully hydrodynamical simulations. These results can thus be considered to be consistent with ours.

## 5 THE METAGALACTIC HYDROGEN IONIZATION RATE

### 5.1 The error budget

We now proceed to place joint constraints on the metagalactic hydrogen ionization rate using independent estimates for several cosmological and astrophysical parameters. We adopt the values listed in Table 3. The values of  $T_0$  and  $\gamma$  are based on the results of Schaye et al. (2000) and we assume the Ly $\alpha$  effective optical depth advocated by Schaye et al. (2003). The cosmological parameters are consistent with the results of Spergel et al. (2003), based on their analysis of the cosmic microwave background anisotropy. Using our scaling relations, we estimate the error in the values of  $\Gamma_{-12}$  from our fiducial simulation, corrected for box size and resolution. The total error is calculated by adding the individual contributions in quadrature, with the percentage error in  $\Gamma_{-12}$  contributed by each parameter listed in Table 4. We make the conservative assumption of an additional numerical uncertainty of 10 per cent to take into account numerical convergence and the modest differences from the numerical simulations of other authors. The total percentage errors in  $\Gamma_{-12}$  are  $[\pm 52, \pm 39, \pm 49]$  per cent at  $z = [2, 3, 4]$ , with the largest contribution coming from the uncertainty in the gas temperature.

**Table 3.** Fiducial parameter values and estimates of their uncertainty. The values listed for gas temperature at mean density  $T_0$  and the effective optical depth  $\tau_{\text{eff}}$  are for  $z = [2, 3, 4]$ .

Parameter	Fiducial values and uncertainties
$T_0$	[11200, 17800, 12500] $\pm$ 5000 K
$\Omega_m$	0.26 $\pm$ 0.04
$\tau_{\text{eff}}$	[0.130 $\pm$ 0.021, 0.362 $\pm$ 0.036, 0.805 $\pm$ 0.070]
$\gamma$	1.3 $\pm$ 0.3
$\Omega_b h^2$	0.024 $\pm$ 0.001
$\sigma_8$	0.85 $\pm$ 0.05
$h$	0.72 $\pm$ 0.04



**Table 4.** Percentage error budget for  $\Gamma_{-12}$  from estimates of various cosmological and astrophysical parameters, listed approximately in order of importance. The total error is obtained by adding the individual errors in quadrature.

Parameter	$z = 2.00$	$z = 3.00$	$z = 4.00$
$T$	$^{+50}_{-22}$ per cent	$^{+23}_{-14}$ per cent	$^{+35}_{-18}$ per cent
$\Omega_m$	$^{+18}_{-13}$ per cent	$^{+19}_{-14}$ per cent	$^{+21}_{-15}$ per cent
$\tau_{\text{eff}}$	$^{+29}_{-19}$ per cent	$^{+18}_{-14}$ per cent	$^{+17}_{-13}$ per cent
Numerical	$\pm 10$ per cent	$\pm 10$ per cent	$\pm 10$ per cent
$\gamma$	$\pm 1$ per cent	$^{+7}_{-9}$ per cent	$^{+12}_{-13}$ per cent
$\Omega_b h^2$	$^{+9}_{-8}$ per cent	$^{+9}_{-8}$ per cent	$^{+9}_{-8}$ per cent
$\sigma_8$	$^{+6}_{-5}$ per cent	$\pm 6$ per cent	$^{+8}_{-7}$ per cent
$h$	$\pm 6$ per cent	$\pm 6$ per cent	$\pm 6$ per cent
Total	$^{+62}_{-36}$ per cent	$^{+39}_{-30}$ per cent	$^{+49}_{-34}$ per cent

There is also a large contribution from the uncertainty in the effective optical depth, especially at  $z = 2$ . Interestingly, the uncertainty in  $\Omega_m$  also gives a substantial contribution to the total error budget. This is primarily due to the sensitivity of  $\Gamma_{-12}$  to  $\Omega_m$  due to changes in the rms fluctuations of the gas density at the Jeans scale. Other uncertainties are less important, in particular  $\Omega_b h^2$ ,  $\sigma_8$  and  $h$ . This contrasts with the conclusion of Tytler et al., who find  $\sigma_8$  is the biggest contribution to the uncertainty in  $\Gamma_{-12}$ . However, they find a stronger dependence of  $\Gamma_{-12}$  on  $\sigma_8$  than we do, and they do not investigate the contribution of uncertainties in  $\Omega_m$  or  $T$  to this error. Note also that inhomogeneities in the UV background may increase estimates of  $\Gamma_{-12}$  by up to 20 per cent if the UV background is

dominated by emission of QSOs (Gnedin & Hamilton 2002; Croft 2004; Meiksin & White 2004). We will conclude in Section 5.2 that QSOs contribute less than half of the ionizing UV background. We will therefore neglect a possible error due to inhomogeneities in the UV background. Using our fiducial model, we find the Ly $\alpha$  effective optical depth of the IGM at  $z = [2, 3, 4]$  is reproduced by  $\Gamma_{-12} = [1.29^{+0.80}_{-0.46}, 0.86^{+0.34}_{-0.26}, 0.97^{+0.48}_{-0.33}]$ .

## 5.2 Comparison with other observational estimates

We compare our results with other observational estimates of  $\Gamma_{-12}$  in Fig. 7. Our estimates are plotted as filled diamonds, with the error bound shown by the dark grey shaded region. The filled triangles show the metagalactic hydrogen ionization rate computed from the updated UV background model of Madau et al. (1999, hereinafter MHR99) (Francesco Haardt, private communication). The values quoted here are smaller by more than a factor of two than those presented in the work of HM96, primarily due to different assumptions about the emissivity of the ionizing sources, and to a lesser extent about the assumed cosmology. The rates are based on the QSO optical luminosity function of Boyle et al. (2000), with a redshift evolution similar to that of MHR99, aside from a steeper evolution for  $z > 3$  to fit data from the SDSS survey (Fan et al. 2001). These values are computed assuming the current cosmological concordance model, and also include the contribution of diffuse radiation from re-processing by the IGM (e.g. HM96). Our data appear to be inconsistent with the IGM being kept ionized by QSOs at  $z \leq 4$ . For comparison, the filled squares give  $\Gamma_{-12}$  calculated using the QSO rate above, plus an additional source in the form of Young Star Forming Galaxies (YSFGs). The YSFG rates are based on the models of Bruzual & Charlot (1993), assuming a Salpeter IMF, a constant star formation rate, an age of 500 Myr,  $Z = 0.2 Z_{\odot}$  and a star formation history as in MHR99. The very uncertain escape fraction is assumed to be  $f_{\text{esc}} = 0.1$ . Note that at low

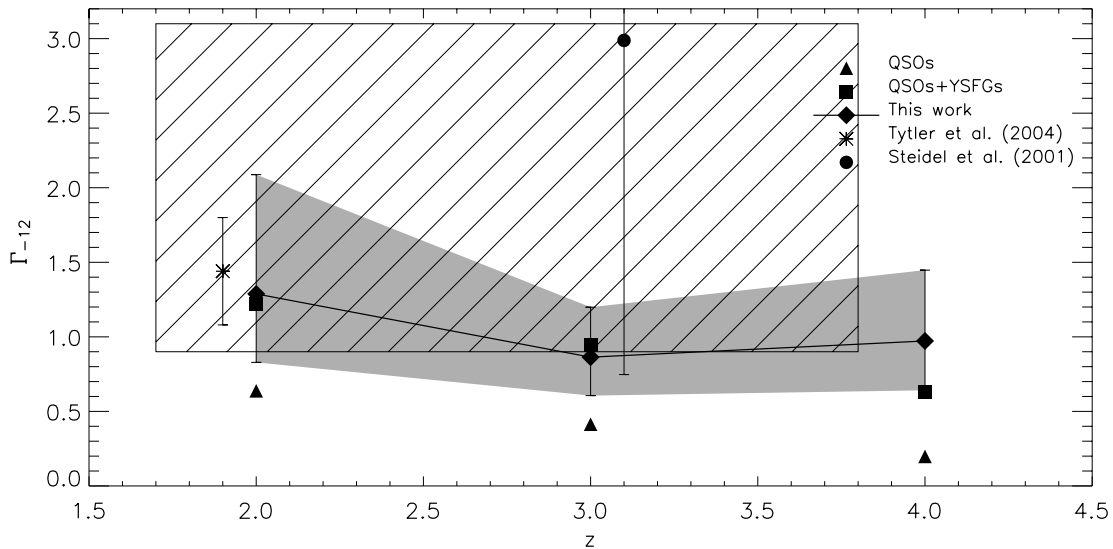


**Figure 7.** Comparison of our best estimate for  $\Gamma_{-12}$  at  $z = [2, 3, 4]$  with constraints from observations. Our data are plotted with filled diamonds, and the grey shaded area shows the error bounds. The filled squares and triangles show the estimated contribution to the metagalactic ionization rate from QSOs+galaxies and QSOs alone, based on estimates from the updated model of Madau et al. (1999) including UV photons from re-processing by the IGM. The hatched box gives the constraint on  $\Gamma_{-12}$  from the proximity effect (Scott et al. 2000) and the estimate from Lyman-break galaxies assuming a global spectral index of  $\alpha = 1.8$  is plotted with a filled circle (Steidel et al. 2001). The data point has been offset from  $z = 3$  for clarity, and the upper error limit is not shown. The star shows the best estimate of  $\Gamma_{-12}$  at  $z = 1.9$  from Tytler et al. (2004), including their errors from the uncertainty in  $\tau_{\text{eff}}$ ,  $\sigma_8$  and  $\Omega_b$ .

redshift the observed value is less than half this (Leitherer et al. 1995; Fernández-Soto, Lanzetta & Chen 2003).

These ionization rates are in good agreement with our results, suggesting that a substantial contribution from galaxies appears to be required at all redshifts. Note, however that there are still substantial uncertainties in the estimates of the ionization rate due to QSOs and galaxies. Hunt et al. (2004), Croom et al. (2004) and Barger et al. (2004) all suggest that the faint end slope of the luminosity function of optically and UV bright QSOs is shallower than the extrapolation from the Boyle et al. data, which may further lower the expected contribution by QSOs. On the other hand, Scott et al. (2004) find that the UV spectrum of low-luminosity QSOs is substantially harder than that of bright QSOs, which may somewhat increase their contribution to the UV background. The main uncertainty in the estimate for the ionization rate due to the UV emission of galaxies is the escape fraction of ionizing photons. However, the improved estimates for the QSO emissivity are so low that there should now be little doubt that the UV background cannot be dominated by QSOs over the full redshift range  $2 < z < 4$ . Aguirre et al. (2004) come to similar conclusions in their study of the Si IV/C IV ratio of the associated metal absorption in Ly $\alpha$  forest spectra.

Constraints on  $\Gamma_{-12}$  from the proximity effect measurements of Scott et al. (2000) are shown by the hatched box, based on a set of 99 moderate resolution QSO spectra. Similar results have been obtained by Cooke et al. (1997). Allowance has been made for variation in the spectral indices of QSOs and differences in systemic redshifts measured from the [O III] or Mg II line and Ly $\alpha$  emission. Our results are consistent with the lower end of these estimates. The filled circle gives the  $\Gamma_{-12}$  we calculate assuming a spectral index of  $\alpha = 1.8$  using the metagalactic ionizing radiation intensity  $J_\nu(912 \text{ \AA})$  inferred from Lyman-break galaxies (LBGs) (Steidel et al. 2001). Steidel et al. quote  $J_\nu(912 \text{ \AA}) \simeq 1.2 \pm 0.3 \times 10^{-21} \text{ erg s}^{-1} \text{ cm}^{-2} \text{ Hz}^{-1} \text{ sr}^{-1}$  at  $z \sim 3$  based on observations of the bluest 25 per cent of LBGs. We offset the data point from  $z = 3$  for clarity, and the upper error limit extends beyond the range of the plot. We estimate the maximum error in this result to be a factor of four to allow for the possibility that the 75 per cent of LBGs that are redder may contribute negligibly to the UV background. Note that Giallongo et al. (2002) found an upper limit to the escape fraction from two bright LBGs that is about a factor four lower than that measured by Steidel et al. There are further uncertainties due to the mean free path of ionizing photons assumed by Steidel et al. and the spectral index that we assumed.

Finally we also plot the value of  $\Gamma_{-12}$  inferred by Tytler et al. (2004) in their study of the Ly $\alpha$  forest at  $z = 1.9$ . The error bars include the uncertainties in  $\tau_{\text{eff}}$ ,  $\sigma_8$  and  $\Omega_b$ , based on scaling from their hydrodynamical simulations.

## 6 CONCLUSIONS

We have examined the dependence of the ionization rate per hydrogen atom on cosmological and astrophysical parameters using hydrodynamical simulations. This is the first time all these parameters have been studied using fully hydrodynamical SPH simulations with high resolution in large boxes. We find that the gas temperature, the effective optical depth  $\tau_{\text{eff}}$  and the mass fraction  $\Omega_m$  have a marked effect upon the hydrogen ionization rate, in addition to the baryon fraction  $\Omega_b$ ,  $\sigma_8$ ,  $\gamma$  and the Hubble constant. We find that  $\Gamma_{-12}$  scales around our fiducial model as

$$\Gamma_{-12} \propto \Omega_m^2 h^3 T^{x_1(z)} \gamma^{x_2(z)} \Omega_m^{x_3(z)} \sigma_8^{x_4(z)} \tau_{\text{eff}}^{x_5(z)}, \quad (10)$$

**Table 5.** The redshift-dependent indices from our scaling relation of  $\Gamma_{-12}$  with several cosmological and astrophysical parameters.

$z$	$T$ $x_1(z)$	$\gamma$ $x_2(z)$	$\Omega_m$ $x_3(z)$	$\sigma_8$ $x_4(z)$	$\tau_{\text{eff}}$ $x_5(z)$
2	-0.68	-0.04	-1.00	-0.90	-1.44
3	-0.62	0.34	-1.04	-0.99	-1.61
4	-0.59	0.55	-1.16	-1.26	-1.68

where we tabulate the indices of equation (10) in Table 5. We stress that this scaling relation is likely to be somewhat model dependent and should not be applied to models with parameters very different from our fiducial model without further checks. However, it does provide a clear picture of the degeneracies that exist between  $\Gamma_{-12}$  and other parameters within our simulations, and is independent of assumptions about the gas distribution, effective equation of state and ionized gas fraction of the low-density IGM. In particular, the Ly $\alpha$  optical depth at fixed rms-fluctuation amplitude  $\sigma_8$  is more strongly dependent on  $\Omega_m$  than the FGPA suggests due to changes in the gas-density distribution. Thermal broadening also produces a deviation from the FGPA scaling for temperature, although this change is much less dramatic. Consequently, we urge caution when using the FGPA scaling relation, especially if comparing models with differing  $\Omega_m$ . We find good agreement with estimates of  $\Gamma_{-12}$  from the Ly $\alpha$  forest opacity by other authors if differences in the assumed cosmological, astrophysical and numerical parameters are taken into account.

In recent years, compelling observational evidence has led to the acceptance of a standard cosmological model which is flat, has low matter density and a substantial contribution of dark energy to the total energy density. Within this ‘concordance’ cosmological model the current generation of hydrodynamical simulations predict values for the metagalactic hydrogen ionization rate, required to reproduce the effective Ly $\alpha$  optical depth of the IGM in the range  $z = 2-4$ , which are about a factor of four larger than those in an Einstein-de Sitter model with the same rms-density-fluctuation amplitude  $\sigma_8$ . The ionization rates estimated from the Ly $\alpha$  forest opacity are more than a factor of two larger than estimates from the integrated flux of optically/UV bright observed QSOs alone. This discrepancy increases with increasing redshift. We confirm the findings of Tytler et al. (2004) at  $z \sim 1.9$  that the estimated ionization rates from simulations of a  $\Lambda$ CDM concordance model are in reasonable agreement with the estimates of the integrated ionizing flux from observed QSOs plus a significant contribution from galaxies as in the model of MHR99. A model where the UV background is dominated by emission from QSOs appears to be inconsistent with the Ly $\alpha$  forest data in the complete redshift range  $2 < z < 4$ . The estimates of the ionization rate are also in agreement with the lower end of the range of estimates from the proximity effect.

There are still many issues that need to be resolved. In particular, better constraints on the thermal history of the IGM are required. Additional physics such as radiative transfer, galactic feedback and metal enrichment may need to be incorporated into simulations in a more realistic fashion. However, our estimate of the errors in  $\Gamma_{-12}$  most probably accounts for the modest changes expected from these processes, suggesting we have obtained a consistent constraint on the metagalactic hydrogen ionization rate.

## ACKNOWLEDGMENTS

We are grateful to Francesco Haardt for making his updated UV background model available to us. This research was conducted

in cooperation with SGI/Intel utilizing the Altix 3700 supercomputer COSMOS at the Department of Applied Mathematics and Theoretical Physics in Cambridge and on the Sun Linux cluster at the Institute of Astronomy in Cambridge. COSMOS is a UK-CCC facility supported by HEFCE and PPARC. We also acknowledge support from the European Community Research and Training Network ‘The Physics of the Intergalactic Medium’. This research was supported in part by the National Science Foundation under Grant No. PHY99-07949. JSB, MGH and MV thank PPARC for financial support. We also thank the referee, Joop Schaye, for a helpful report.

## REFERENCES

- Abel T., Haehnelt M. G., 1999, *ApJ*, 520, L13  
 Abel T., Anninos P., Zhang Y., Norman M. L., 1997, *New Astron.*, 2, 181  
 Aguirre A., Schaye J., Kim T.-S., Theuns T., Rauch M., Sargent W. L. W., 2004, *ApJ*, 602, 38  
 Bajtlik S., Duncan R. C., Ostriker J. P., 1988, *ApJ*, 327, 570  
 Barger A. J., Cowie L. L., Mushotzky R. F., Yang Y., Wang W.-H., Steffen A. T., Capak P., 2004, preprint (astro-ph/0410527)  
 Bechtold J., 1994, *ApJS*, 91, 1  
 Bernardi M. et al., 2003, *AJ*, 125, 32  
 Bi H. G., Davidson A. F., 1997, *ApJ*, 479, 523  
 Bi H. G., Börner G., Chu Y., 1992, *A&A*, 266, 1  
 Bolton J., Meiksin A., White M., 2004, *MNRAS*, 348, L43  
 Boyle B. J., Shanks T., Croom S. M., Smith R. J., Miller L., Loaring N., Heymans C., 2000, *MNRAS*, 317, 1014  
 Bruscoli M., Ferrara A., Marri S., Schneider R., Maselli A., Rollinde E., Aracil B., 2003, *MNRAS*, 343, 51  
 Bruzual A. G., Charlot S., 1993, *ApJ*, 405, 538  
 Bryan G. L., Machacek M. E., 2000, *ApJ*, 534, 57  
 Cen R., 1992, *ApJS*, 78, 341  
 Cooke A. J., Espey B., Carswell B., 1997, *MNRAS*, 284, 552  
 Couchman H. M. P., Thomas P. A., Pearce F. R., 1995, *ApJ*, 452, 797  
 Croft R. A. C., 2004, *ApJ*, 610, 642  
 Croom S. M., Smith R. J., Boyle B. J., Shanks T., Miller L., Outram P. J., Loaring N. S., 2004, *MNRAS*, 349, 1397  
 Desjacques V., Nusser A., Haehnelt M. G., Stoehr F., 2004, *MNRAS*, 350, 879  
 Eisenstein D. J., Hu W., 1999, *ApJ*, 511, 5  
 Fan X. et al., 2001, *ApJ*, 122, 2833  
 Ferland G. J., Peterson B. M., Horne K., Welsh W. F., Nahar S. N., 1992, *ApJ*, 387, 95  
 Fernández-Soto A., Lanzetta K. M., Chen H.-W., 2003, *MNRAS*, 342, 1215  
 Giallongo E., Cristiani S., D’Odorico S., Fontana A., 2002, *ApJ*, 568, L9  
 Gnedin N. Y., 1998, *MNRAS*, 299, 392  
 Gnedin N. Y., Hamilton A. J. S., 2002, *MNRAS*, 334, 107  
 Gnedin N. Y., Hui L., 1998, *MNRAS*, 296, 44  
 Gunn J. E., Peterson B. A., 1965, *ApJ*, 142, 1633  
 Haardt F., Madau P., 1996, *ApJ*, 461, 20 (HM96)  
 Haehnelt M. G., Madau P., Kudritzki R., Haardt F., 2001, *ApJ*, 549, L151  
 Hernquist L., Katz N., Weinberg D. H., Miralda-Escudé J., 1996, *ApJ*, 457, L51  
 Hui L., Gnedin N., 1997, *MNRAS*, 292, 27  
 Hui L., Haiman Z., Zaldarriaga M., Alexander T., 2002, *ApJ*, 564, 525  
 Hunt M. P., Steidel C. C., Adelberger K. L., Shapley A. E., 2004, *ApJ*, 605, 625  
 Katz N., Weinberg D. H., Hernquist L., 1996, *ApJS*, 105, 19  
 Kim T.-S., Cristiani S., D’Odorico S., 2001, *A&A*, 373, 757  
 Kim T.-S., Carswell R. F., Cristiani S., D’Odorico S., Giallongo E., 2002, *MNRAS*, 335, 555  
 Kirkman D., Tytler D., 1997, *ApJ*, 484, 672  
 Leitherer C., Ferguson H. C., Heckman T. M., Lowenthal J. D., 1995, *ApJ*, 454, L19  
 Lu L., Sargent W. L. W., Womble D. S., Takada-Hidai M., 1996, *ApJ*, 472, 509  
 Madau P., Haardt F., Rees M. J., 1999, *ApJ*, 585, 34 (MHR99)  
 McDonald P., Miralda-Escudé J., 2001, *ApJ*, 549, L11  
 McDonald P., Miralda-Escudé J., Rauch M., Sargent W. L. W., Barlow T. A., Cen R., 2001, *ApJ*, 562, 52  
 Meiksin A., White M., 2001, *MNRAS*, 324, 141  
 Meiksin A., White M., 2003, *MNRAS*, 342, 1205  
 Meiksin A., White M., 2004, *MNRAS*, 350, 1107  
 Miralda Escudé J., Cen R., Ostriker J. P., Rauch M., 1996, *ApJ*, 471, 582  
 Norman M. L., Bryan G. L., 1999, in Miyama S.M., Tomisaka K., Hanawa T., eds, *Astrophys. & Space Sci. Lib.*, Vol. 240: Numerical Astrophysics. Springer, Berlin, p. 19  
 O’Shea B. W., Nagamine K., Springel V., Hernquist L., Norman M. L., 2003, preprint (astro-ph/0301265)  
 Press W. H., Rybicki G. B., Schneider D. P., 1993, *ApJ*, 414, 64  
 Rauch M., 1998, *ARA&A*, 36, 267  
 Rauch M. et al., 1997, *ApJ*, 489, 7  
 Reimers D., Kohler S., Wisotzki L., Groote D., Rodriguez-Pascual P., Wamsteker W., 1997, *A&A*, 327, 890  
 Ricotti M., Gnedin N., Shull M., 2000, *ApJ*, 534, 41  
 Schaye J., Theuns T., Rauch M., Efstathiou G., Sargent W.L.W., 2000, *MNRAS*, 318, 817  
 Schaye J., Aguirre A., Kim T.-S., Theuns T., Rauch M., Sargent W.L.W., 2003, *ApJ*, 596, 768  
 Scott J., Bechtold J., Dobrzycki A., Kulkarni V. P., 2000, *ApJS*, 130, 67  
 Scott J. E., Kriss G. A., Brotherton M., Green R. F., Hutchings J., Shull J. M., Zheng W., 2004, *ApJ*, 615, 135  
 Sokasian A., Abel T., Hernquist L., 2003, *MNRAS*, 340, 473  
 Songalia A., Cowie L. L., 2002, *AJ*, 123, 2183  
 Spergel D. N. et al., 2003, *ApJS*, 148, 175  
 Springel V., Hernquist L., 2002, *MNRAS*, 333, 649  
 Springel V., Hernquist L., 2003, *MNRAS*, 339, 289  
 Springel V., Yoshida N., White S. D. M., 2001, *New Astron.*, 6, 79  
 Steidel C. C., Pettini M., Adelberger K. L., 2001, *ApJ*, 546, 665  
 Theuns T., Leonard A., Efstathiou G., Pearce F., Thomas P. A., 1998, *MNRAS*, 301, 478  
 Theuns T., Schaye J., Haehnelt M. G., 2000, *MNRAS*, 315, 600  
 Theuns T., Viel M., Kay S., Schaye J., Carswell B., Tzanavaris P., 2002, *ApJ*, 578, L5  
 Tytler D. et al., 2004, *ApJ*, 617, 1  
 Weinberg D. H., Hernquist L., Katz N., Croft R., Miralda-Escudé J., 1997, in Petitjean P., Charlot S., eds, *Proc. 13th IAP Colloq., Structure and Evolution of the Intergalactic Medium*. Editions Frontières, Paris, p. 133  
 Weinberg D. et al., 1999, in Banday A. J., Sheth R. K., da Costa L. N., eds, *Evolution of Large Scale Structure: from Recombination to Garching*. PrintPartners Ipskamp, Enschede, p. 346  
 Viel M., Haehnelt M. G., Carswell R. F., Kim T.-S., 2004a, *MNRAS*, 349, L33  
 Viel M., Haehnelt M. G., Springel V., 2004b, *MNRAS*, 354, 184  
 Zhang Y., Anninos P., Norman M. L., 1995, *ApJ*, 453, L57  
 Zhang Y., Meiksin A., Anninos P., Norman M. L., 1998, *ApJ*, 495, 63

This paper has been typeset from a  $\text{\TeX}/\text{\LaTeX}$  file prepared by the author.